Waste Management and Research, Vol. 36, Issue 11, (2018), pp. 1043-1048
DOI:10.1177/0734242X18804642

Electrochemically generated bimetallic reductive mediator $Cu^{1+}[Ni^{2+}(CN)_4]^{1-}$ for the degradation of CF_4 to ethanol by electro-scrubbing

G. Muthuraman[a], A.G. Ramu[a], Y. H. Cho[b], E.J. McAdam[c], and I. S. Moon[a]*

[a]Department of Chemical Engineering, Sunchon National University,

#255 Jungangno, Suncheon 540-742, Jeollanam-do, Rep. of Korea.

[b]Korea Atomic Energy Research Institute, Yuseong P.O Box 105, Daejeon, Rep. of Korea

[c]Cranfield Water Science Institute, Cranfield University, Building 39, MK43 0AL, UK

**Corresponding author(ismoon@sunchon.ac.kr)*

Abstract

Remediation of electronic gas CF_4 by using commercially available technologies ended up with another kind of greenhouse gas and corrosive side products. This investigation aimed to develop CF_4 removal at room temperature with formation of useful product by attempting an electrogenerated $Cu^{1+}[Ni^{2+}(CN)_4]^{1-}$ mediator. In the initial electrolysis of bimetallic complex at anodized Ti cathode demonstrated the $Cu^{1+}[Ni^{2+}(CN)_4]^{1-}$ formation, which was confirmed by additional ESR results. The degradation of CF_4 followed mediated electrochemical reduction (MER) by electrogenarated $Cu^{1+}[Ni^{2+}(CN)_4]^{1-}$. The removal efficiency of CF_4 was achieved 95% by this present electroscrubbing process at room temperature. Through the spectral results of online and offline FTIR analyzer either in gas or in solution phase demonstrated that the formed product during the removal of CF_4 by electrogenerated $Cu^{1+}[Ni^{2+}(CN)_4]^{1-}$ at electroscrubbing was ethanol (CH_3CH_2OH) with small amount of trifluoroethane (CF_3CH_3) intermediate.

Key words: Bimetallic mediator, $Cu^{1+}[Ni^{2+}(CN)_4]^{1-}$, MER, CF_4 degradation; Ethanol formation

Introduction

The so called electronic gases (CF_4, NF_3 and SF_6) become inevitable to human life in the both extreme ways either positive by new sophisticated electronic goods or negative by environmental pollution. The increasing number of electronic gas pollutions not only forced to innovate new removal technologies but also due to the currently and commercially available two methods such as combustion (Rittmeyer and Vehlow (1993); Lee et al., (1996)) and plasma arc (Lee et al., (2005); Gal et al., (2003)) were produced mostly another greenhouse gas CO_2 and its derivatives (COF_2, CO, H_2O),with HF (Xu et al., (2007); Gandhi and Mok (2012); Narengerile et al., (2010); Zhang et al., (2005)) depending upon the carrier gas. In recent past, catalytic combustion has attracted some additional interest towards more practical level (Xu et al., (2011); Takita et al., (1999)), especially hydrolytic combustion possess less Gibbs energy (−150 kJ/mol). Unfortunately, the final product that obtained is highly corrosive hydrofluoric acid (HF) as shown in reaction 1, that produced HF led to deactivation of the used catalyst (Farris et al., (1992)). In order to minimize the deactivation of catalyst, binary metal catalyst were attempted, with the idea of C-F bond breaking at Lewis-acid catalysts that formed metal fluoride can be easily hydrolyzed, to degrade CF_4 by hydrolytic combustion process (El-Bahy et al., (2003); Takita et al., (1999)-2; Song et al., (2013)). El-Bahy et al., (2003) have attempted various bimetal combinations and found Ga-Al and Ni-Al oxide catalyst were stable from HF deactivation. Xu et al., (2007) have found CF_4 conversion to CO_2 with minimized deactivation of γ-Al_2O_3 catalysts by addition of Zn, Ni, Mg, Sr and Ba metals. Song et al., (2013) were developed Ce/Al_2O_3 binary catalyst that was not effectively performed on removal of CF_4 though the catalyst found stable. In result, the catalytic combustion also produces

another greenhouse gas CO_2 in CF_4 decomposition process.

$$CF_4 + 2H_2O \longrightarrow CO_2 + 4HF\ (\Delta G = -150\ kJ/mol) \quad \text{--- (1)}$$

At the same time, electrochemical technique offers degradation of chloro fluoro carbons (CFCs) can be done at room temperature and release non-fluoro compounds with absence of additional greenhouse gas CO_2 (Sonoyama and Sakata (1998); Cabot et al., (2004); Wagoner and Peters (2013)). Sonoyama and Saakta (1998)-2 have performed metal (Cu) supported gas diffusion electrode on degradation of $CClF_3$ (CFC-13) that results in methane formation and on Ag supported gas diffusion electrode tend to form CHF_3. In solution phase electrochemical degradation process, direct reduction of CFCs in acetonitrile (Schizodimou et al., (1999)) and DMF (Wagoner et al., (2012)) on different metal electrodes have been reported, with the idea of solubility of CFCs, to produce main products CF_2CF_2, CH_2F_2, CH_3F, CF_2CFCl and $CHCF_3$ that are used as raw material in production of polymers and refrigerants. Cabot et al., (2003) have used methanol water mixture medium to degrade CFC-11 and CFC-113 using Pb cathode with Pd contained gas diffusion anode by constant potential electrolysis, where complete or partially dehalogenated product were achieved depending on the Pd contents. Taylor-Smith and Sayres (1999) have found through fundamental electrochemical studies on selective site-specific PFCs compounds that the reduction reaction follows radical reaction with carbanion formation with subsequent oligomeric products such as C_3H_8, C_3F_8, and CH_4 from CF_4 and etc.,. Note that most of the electrochemical studies to degrade CFCs in aprotic medium or combination of aprotic and protic solvents using CV or constant potential electrolysis, none were performed in only aqueous medium and constant current in degradation process. Very recently, CF_4 removal have reported by our group using mediated electrochemical reduction (MER) in aqueous KOH medium at room temperature by electrochemically generated mediator

Co^{1+} at electro-scrubbing process (Muthuraman and Moon (2017)). Ethanol and HF were the products found in the Co^{1+} MER of CF_4 (Muthuraman and Moon (2017)). As well explained in the literature that HF formation will affect the removal of CF_4 process, the HF formation in our report may reduce the pH in long term electrolysis that will affect mediator generation process finally removal efficiency will be reduced. In order to avoid HF formation in the removal process, here in, we have attempted a binary metal complex or bimetallic complex, as reported in catalytic combustion process for catalysts activation, in MER of CF_4.

In the present investigation, a bimetallic complex $Cu^{2+}[Ni^{2+}(CN)_4]$ was used as mediator precursor in degradation of CF_4 gas. A cathodic half-cell in a divided electrolytic cell was used to generate a low valent active mediator generation in 10 M KOH medium by constant current method. The electrolytic reduction of $Cu^{2+}[Ni^{2+}(CN)_4]$ was performed on anodized Ti or TiO_2 cathodeconducted in 10 M KOH on an anodized Ti cathode. The oxidation/reduction potential (ORP) of the Cu^{2+} and Ni^{2+} in the dissolved electrolyzed solution during electrolysis were taken as indication and quantification, by potentiometric titration separately, for the low oxidation state active mediator formation. Additional, ESR analysis was used to support in differentiation of Cu^{2+} or Ni^{2+} reduction in the electrolyzed solution. The CF_4 degradation was carried out at electro-scrubbing where the CF_4 was fed continuously at a controlled rate and concentration through the bottom of the scrubber and subsequently the spent bimetallic complex was sent to cathodic half-cell to generate low oxidation state active mediator. The CF_4 removal efficiencies were monitored using an online Fourier transform infrared (FTIR) gas analyzer. Solution phase and gas phase analyses were conducted to find the final product.

Experimental methods

Preparation of mediator precursor

$Cu^{2+}[Ni^{2+}(CN)_4]$ was prepared, as per the literature procedure (Chippindale et al., (2015)). In brief, $Cu^{2+}(NO_3)_2.3H_2O$ and $Ni^{2+}(CN)_4^{2-}$ were added in 200 ml water with the mole ratio of 1:4 Cu^{2+} to Ni^{2+}. A light blue precipitate formed slowly with constant stirring, which was separated by filtration, washed several times with water, and dried in a desiccator prior to use. $Ni^{2+}(CN)_4^{2-}$ was prepared using existed literature procedure (Fernclius et al., (2007)). Briefly, $Ni^{2+}(NO_3)_2.6H_2O$ was taken with 1:4 mole ratio (Ni^{2+} to cyanide) to KCN, which is already dissolved in 200 ml cooled water (extreme care was taken when handling the KCN during complex preparation due to highly dangerous to human). To this reaction solution, an equal volume of chilled alcohol was then added. The resulting thin orange platelets was filtered rapidly, washed with cold alcohol, recrystallized in ethanol, dried in a vacuum desiccator, and stored in an air-tight brown bottle.

Setup and procedure for mediator generation and degradation

A divided flow-through electrolytic cell was used, as in our previous publication (Muthuraman and Moon (2017)), with suitable additional conditions, as shown in Fig.1. Briefly, a 4 cm^2 working electrode area capacity thin layer plate and frame divided cell (divided with Nafion324) was connected to catholyte (200 ml of mediator precursor in 10 M KOH) and anolyte (200 ml of 5 M H_2SO_4) glass tanks through a polycarbon tubing. So that the anolyte and catholyte were able to circulate (using peristaltic pumps) through the respective anode and cathode compartments. The electrolysis experiments were conducted in constant current mode using a DC power supply. All solutions were prepared using reverse osmosis purified water (Human Power III plus, South Korea) with a resistivity of 18 MΩ-cm.

For the electro-scrubbing process, a 50 cm_2 electrode area capacity divided plate and frame electrochemical cell was connected to a 40 cm high and 5.5 cm (i.d) column packed with 1 cm^2 of Teflon tubes as the packing material on top of the catholyte tank (1 L capacity),as our previous published literature (Muthuraman and Moon (2017)). The electrolyte solutions (500 ml) were circulated continuously to flow through the electrolytic cell at different flow rates (1 to 5 L min^{-1}) using magnetic pumps. The catholyte solution as scrubbing solution (electrolyzed mediator in a KOH solution) was pumped separately into the scrubber column at a flow rate of 3 L min^{-1}. CF_4 gas (from RIGAS (1000 ppm), Korea) and N_2 mixtures, which were obtained by the controlled mixing of air and CF_4 gas using mass flow controllers (MFCs), were introduced to the bottom of the scrubber at a set gas flow rate. An online gas analyzer (FTIR) was attached at scrubber exit to facile the instantaneous degradation measurements. Prior to each electrolysis experiment, the Ti electrode (cathode) was pretreated by anodization (for the partially anodized TiO_2 electrode) process separately in 0.1 M KNO_3 at a constant current of 1 A for 5 min. All experiments were conducted at room temperature (20 ± 2 ºC).

Quantification of mediator ion

The electrolyzed solution contained Cu^{1+} or Ni^{1+} concentrations were determined using a potentiometric titration method (Muthuraman and Moon (2017)). In the present case, the electrolyzed sample solution was titrated against a standard $Fe^{3+}(CN)_6$ (From Sigma Aldrich, USA) solution (0.001 M) and monitor the potential variation using an ORP (oxidation/reduction potential) electrode (EMC 133, 6 mm Pt sensor electrode and Ag/AgCl reference electrode containing a gel electrolyte) connected to an iSTEK multimeter. The initial catholyte ($Cu^{2+}[Ni^{2+}(CN)_4]$) solution potential was approximately -170 mV, which then decreased as electrolysis progressed at a constant current density to reach approximately -400

mV. By titration against 0.001 M $Fe^{3+}(CN)_6$, the initial ORP value can be attained that Fe^{3+} concentration can be used to derive the concentration of Cu^{1+}, as shown eqn. 2

Concentration of Cu^{1+} with respect to the initial Cu^{2+} in $Cu^{2+}[Ni^{2+}(CN)_4]$ =

$$(C_{Cu2+} \times C_{Cu1+})/C_{Cu2+-Ni2+} \quad \text{--- (2)}$$

Analysis

The gas phase online analysis was performed using online FTIR gas analyzer (from MIDAC Corporation, USA). The solution phase sample analysis was carried out by attenuated total reflectance – Fourier transform infrared (ATR-FTIR, Thermo scientific, Nicolet iS5, USA) spectroscopy using a 2 μL drop of the reaction sample on the diamond sample holder to derive products. To understand the low oxidation state of the metal ion its influence in CF_4 degradation process, ESR spectrometer with focused light of a 1000 W high-pressure Hg lamp through an aqueous filter. The ESR spectra were measured at 143 K with a JEOL X-band spectrometer (JES-RE1XE) using an attached VT (Variable Temperature) apparatus under non saturating microwave power conditions.

Results and discussion

Generation of reductive mediator

Fig.2 shows the ORP value changes during electrolysis of different mediator precursor contained electrolyzed solution ($Cu^{2+}(OH)_4^{2-}$, $Ni^{2+}(CN)_4^{2-}$, and $Cu^{2+}[Ni^{2+}(CN)_4]$). The ORP values of the electrolyzed solution reached a maximum of -450 mV for $Cu^{2+}(OH)_4^{2-}$ in 1h electrolysis (Fig.2 curve a). In the case of $Ni^{2+}(CN)_4^{2-}$ electrolysis, the ORP value was reached to nearly -800 mV in 1h (Fig.2 curve c). On the other hand, the ORP value of $Cu^{2+}[Ni^{2+}(CN)_4]$

electrolyzed solution shows ~ – 500 mV in 1h electrolysis time indicating that Cu^{2+} is reduced instead of Ni^{2+} reduction in the heterobimetallic complex. In order to confirm whether Cu^{2+} is reduced, the electrolyzed solution of $Cu^{2+}[Ni^{2+}(CN)_4]$ was analyzed by ESR that results are shown in Fig.3. The ESR spectra shows symmetrical with identical g_{xx} and g_{yy} values, A_{xx} and A_{yy} and a large A_{zz} value, which is greater than 140 G confirms Cu^{2+} complex with a square-planar geometry (Savelieff et al., (2008)) (Fig.3 curve a). At the same time the electrolyzed $Cu^{2+}[Ni^{2+}(CN)_4]$ samples shows reduced intensity without change in symmetrical values evidences the Cu^{1+} formation with square planar geometry (Fig.3 curve b). The insert figure of Fig.4 shows Cu^{1+} concentration variation with electrolysis time, where Cu^{1+} concentration obtained was maximum of 3.1 mM out of 12 mM in the bimetallic complex at given conditions.

CF_4 degradation

Once reached the Cu^{1+} concentration to around 3 mM by electrolysis, the electrolyzed solution of $Cu^{1+}/Cu^{2+}[Ni^{2+}(CN)_4]$ was pumped into the scrubbing column via top of the scrubbing column then after 10 ppm of CF_4 was injected at 0.2 L min^{-1} gas flow rate into the bottom of the scrubbing column, while electrolysis was continued to regenerate the Cu^{1+}. The obtained results under these conditions are shown in Fig.4, there found almost o ppm at scrubber exit at initial timings and then 0.2 ppm of CF_4 started come out at the scrubber exit in 1h duration, which is equal to the removal efficiency of 96% that explains CF_4 removal at room temperature by the electrogenerated $Cu^{1+}[Ni^{2+}(CN)_4]$ is possible. Noteworthy here that CF_4 absorption in to 10 M KOH solution attained saturation in 5 min (Muthuraman and Moon (2017)). The Cu^{1+} concentration variation during the CF_4 removal process can authenticate whether the electrogenerated Cu^{1+} is involved in the CF_4 removal reaction. The insert figure of Fig.4 shows that there is a Cu^{1+} concentration decrease from 3.1 mM to 2.1 mM initially then

decreases further to 1.2 mM in 1h CF_4 removal time, which is clearly indicate the CF_4 removal reaction follow MER by electrogenerated $Cu^{1+}[Ni^{2+}(CN)_4]^{1-}$.

Fig. 5A shows CF_4 removal at different gas flow rates. Initially there shows almost 100% removal of CF_4 up to 1 L min^{-1}, but decreased to 55% with increasing gas flow rate at later removal timings. The decrease in CF_4 removal efficiency at high gas flow rate could be due the feed CF_4 is higher than the generation rate of Cu^{1+}. In the case of feed concentration variation, up to 10 ppm of CF_4 feed shows almost 95% removal efficiency (Fig.5B curve a & b). Beyond 10 ppm of CF_4 shows removal efficiency of nearly 40% at initial stages but then decreased to 0% removal efficiency in 30 min (Fig.5B curve c) explains Cu^{1+} generation rate is not at all meet with feed CF_4 concentration or 10 ppm of CF_4 feed is more optimum at given conditions.

Product identification

According with Fig.4, almost 95% of CF_4 removal has been achieved from the beginning of the removal process, but no products has been noticed at scrubber in first 30 min (Fig.6). After 30 min, there found a huge concentration ethanol (CH_3CH_2OH) suddenly emerged at scrubber exit around 125 ppm Fig.6 curve a). In similar time interval, trifluoroethane (CH_3CF_3) started exit around 10 ppm (Fig.6 curve b). Surprisingly, no HF is coming out of scrubber, interestingly no greenhouse gases also found in exit gas (Fig.6 curve c). Note that ethanol and HF have started produced from the beginning of the removal process while electrogenerated Co^{1+} mediator used to remove CF_4 gas (Muthuraman and Moon (2017)). The CF_4 removal process follow mediated degradation to soluble products that products came out after a saturation point attained, which could be the reason for the late exit of CH_3CH_2OH and CH_3CF_3. The scrubbing solution underwent an ATR-FTIR analysis after the electro-scrubbing process was completed that reaction solution revealed only CH_3CH_2OH presence (-

O-H and -C-O stretching frequencies well matched with instrument library CH_3CH_2OH sample) in solution (Fig.7), confirming that the reaction product is CH_3CH_2OH. Many electrochemical reports have shown that CFCs form CH_4 and fluorine reduced derivatives such as CF_3CH, CH_2F_2, CH_3F, CF_2CFCl (Schizodimou et al., (1999); Wagoner et al., (2012); Cabot et al., (2003); Taylor-Smith and Sayres (1999)), but found no report to form CH_3CH_2OH during degradation of CF_4. Very recently, direct ethanol formation on copper electrode during reduction of CO_2 through the carbon dioxide dimer formation (Song et al., (2016); Kuhl et al., (2012)). Similarly, carbon tetrafluoride dimer could have formed via electrogenerated Cu^{1+} that might have easily hydroxylated to ethanol, because of the scrubbing solution is 10 M KOH, as shown by proposed scheme 1. The possibility of dimerization confirmed by the additional product CF_3CH_3 (Fig.6 curve b) found at scrubber exit that may be due to incomplete reaction or intermediate formation.

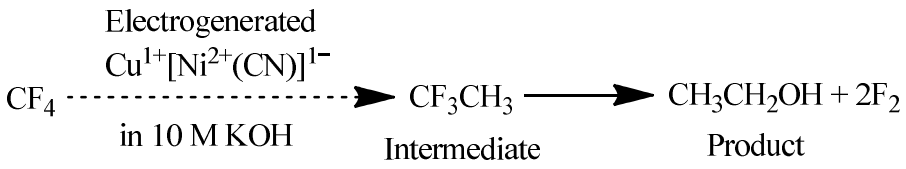

Scheme 1 Plausible reaction pathway for CF_4 degradation to ethanol

Conclusions

We have demonstrated through this investigation that the electrogenerated $Cu^{1+}[Ni^{2+}(CN)_4]^{1-}$ was successfully degraded CF_4 to ethanol without forming HF. The electrogeneration of Cu^{1+} from the bimetallic complex of $Cu^{2+}[Ni^{2+}(CN)_4]$ was identified and confirmed by ORP variation of ESR analysis. Cu^{1+} concentration variation during injection of the CF_4 into the scrubber column or CF_4 removal process confirms the mediated reduction. The

online and offline FTIR analyzer results demonstrate CH_3CH_2OH is a final product along with an intermediate or incomplete product CF_3CH_3 during the degradation of CF_4 by using the electrogenerated $Cu^{1+}[Ni^{2+}(CN)_4]^{1-}$ in highly KOH medium.

Acknowledgement

This study was supported by the National Research Foundation of Korea (NRF) funded by Ministry of Engineering Science and Technology (MEST) from the Korean government (Grant No. NRF-2017R1A2A1A05001484).

References

Cabot P L, Segarra L, and Casado J (2003) Electrodegradation of Chlorofluorocarbons 11 and 113 at Small Concentrations in Closed Cells, *Electrochem. Solid-State Lett.* 6(3): B15-B18.

Cabot P L, Segarra L, and Casado J (2004) Electrodegradation of Chlorofluorocarbons in a Laboratory-Scale Flow Cell with a Hydrogen Diffusion Anode, *J. Electrochem. Soc.* 151(2): B98-B104.

Chippindale A M, Hibble S J, Marelli E, Bilbe E J, Hannon A C, and Zbiri M (2015) Chemistry and Structure by Design: Ordered $CuNi(CN)_4$ Sheets with Copper(II) in a Square-Planar Environment, *Dalton Transactions* 44(28): 12502-12506.

El-Bahy Z M, Ohnishi R, and Ichikawa M (2003) Hydrolysis of CF_4 over Alumina-Based Binary Metal Oxide Catalysts, *Appl. Catal. B* 40(2): 81-91.

Farris M M, Klinghoffer A A, RosSnl J A, and Tevault D E (1992) Deactivation of a Pt/Al_2O_3 Catalyst During the Oxidation of Hexafluoropropylene, *Catalysis Today* 11(4): 501-

516.

Fernelius W C, Burbage J J, and Ballou N E (2007) Potassium Tetracyanonickelate(II), in: Inorganic Syntheses, John Wiley & Sons, Inc., pp. 227-228.

Gal A, Ogata A, Futamura S, and Mizuno K (2003) Mechanism of the Dissociation of Chlorofluorocarbons During Nonthermal Plasma Processing in Nitrogen at Atmospheric Pressure, *The Journal of Physical Chemistry A* 107(42): 8859-8866.

Gandhi M S, and Mok Y S (2012) Decomposition of Trifluoromethane in a Dielectric Barrier Discharge Non-Thermal Plasma Reactor, *J. Environ. Sci. (Beijing, China)* 24(7): 1234-1239.

Kuhl K P, Cave E R, Abram D N, and Jaramillo, T F (2012) New Insights into the Electrochemical Reduction of Carbon Dioxide on Metallic Copper Surfaces, *Energy & Environmental Science* 5(5): 7050-7059.

Lee C W, Ryan J V, Hall R E, Kryder G D, and Springsteen B R (1996) Effects of Copper Contamination on Dioxin Emissions from Cfc Incineration, *Combustion Science and Technology*, 116-117(1-6): 455-478.;l;k

Lee H M, Chang M B, and Lu R F (2005) Abatement of Perfluorocompounds by Tandem Packed-Bed Plasmas for Semiconductor Manufacturing Processes, *Ind. Eng. Chem. Res.* 44(15): 5526-5534..

Muthuraman G, and Moon I S (2017) Innovative Reductive Remediation of Carbon Tetrafluoride at Room Temperature by Using Electrogenerated Co^{1+}, *J. Hazard. Mater.* 325: 157-162.

Narengerile Saito H, and Watanabe T (2010) Decomposition Mechanism of Fluorinated Compounds in Water Plasmas Generated under Atmospheric Pressure, *Plasma Chem.*

Plasma Process. 30(6): 813-829.

Rittmeyer C, and Vehlow J (1993) Decomposition of Organohalogen Compounds in Municipal Solid Waste Incineration Plants. Part I: Chlorofluorocarbons, *Chemosphere* 26(12): 2129-2138.

Savelieff M G, Wilson T D, Elias Y, Nilges M J, Garner D K, and Lu Y (2008) Experimental Evidence for a Link among Cupredoxins: Red, Blue, and Purple Copper Transformations in Nitrous Oxide Reductase, *Proceedings of the National Academy of Sciences* 105(23): 7919-7924.

Schizodimou A, Kyriacou G, and Lambrou C (1999) Electrochemical Reduction of Dichlorodifluoromethane in Acetonitrile Medium to Useful Fluorinated Compounds, *J. Electroanal. Chem.* 471(1): 26-31.

Song J-Y, Chung S-H, Kim M-S, Seo M-g, Lee Y-H, Lee K-Y, and Kim J-S (2013) The Catalytic Decomposition of CF_4 over Ce/Al_2O_3 Modified by a Cerium Sulfate Precursor, *J. Mol. Catal. A: Chem.* 370: 50-55.

Song Y, Peng R, Hensley D K, Bonnesen P V, Liang L, Wu Z, Meyer H M, Chi M, Ma C, Sumpter B G, and Rondinone A J (2016) High-Selectivity Electrochemical Conversion of CO_2 to Ethanol Using a Copper Nanoparticle/N-Doped Graphene Electrode, *Chemistry Select* 1(19): 6055-6061.

Sonoyama N, and Sakata T (1998)-2 Electrochemical Hydrogenation of CFC-13 Using Metal-Supported Gas Diffusion Electrodes, *Environ. Sci. Technol.* 32(24): 4005-4009.

Sonoyama N, and Sakata T (1998) Electrochemical Decomposition of CFC-12 Using Gas Diffusion Electrodes, *Environ. Sci. Technol.* 32(3): 375-378.

Takita Y, Morita C, Ninomiya M, Wakamatsu H, Nishiguchi H, and Ishihara T (1999)-2

Catalytic Decomposition of CF_4 over $AlPO_4$-Based Catalysts, *Chem. Lett.* (5): 417-418.

Takita Y, Ninomiya, M., Miyake, H., Wakamatsu, H., Yoshinaga, Y. and Ishihara, T. (1999), Catalytic Decomposition of Perfluorocarbons Part II. Decomposition of CF_4 over $AlPO_4$-Rare Earth Phosphate Catalysts, *Physical Chemistry Chemical Physics* 1(18): 4501-4504.

Taylor-Smith R E, and Sayres D (1999) Electrochemical Routes to Perfluoro Compound Abatement, *Proc. - Electrochem. Soc.* 99-8(Environmental Issues in the Electronics and Semiconductor Industries): 116-125.

Wagoner E R, and Peters D G (2013) Electrocatalytic Reduction of 1,1,2-Trichloro-1,2,2-Trifluoroethane (CFC-113) at Silver Cathodes in Organic and Organic-Aqueous Solvents, *J. Electrochem. Soc.* 160(10): G135-G141.

Wagoner E R, Hayes J L, Karty J A, and Peters D G (2012) Direct and Nickel(I) Salen-Catalyzed Reduction of 1,1,2-Trichloro-1,2,2-Trifluoroethane (CFC-113) in Dimethylformamide, *J. Electroanal. Chem.* 676: 6-12.

Xu X-F, Jeon J Y, Choi M H, Kim H Y, Choi W C, and Park Y-K (2007) The Modification and Stability of Γ-Al_2O_3 Based Catalysts for Hydrolytic Decomposition of CF_4, *J. Mol. Catal. A: Chem.* 266(1-2): 131-138.

Xu X, Niu X, Fan J, Wang Y, and Feng M (2011) CF_4 Decomposition without Water over a Solid Ternary Mixture Consisting of NaF, Silicon and One Metal Oxide, *J. Nat. Gas Chem.* 20(5): 543-546.

Zhang H, Ng C F, and Lai S Y (2005) Catalytic Decomposition of Chlorodifluoromethane (HCFC-22) over Platinum Supported on TiO_2–ZrO_2 Mixed Oxides, *Applied Catalysis B: Environmental* 55(4): 301-307.

Figure captions

Fig.1 Schematic experimental setup used to degrade CF_4 at wet-scrubber by electrochemically generated $Cu^{1+}[Ni^{2+}(CN)_4]^{1-}$

Fig.2 Oxidation/reduction potential (ORP) variation during electrolysis of different mediator precursors in 10 M KOH solution: (a) 50 mM $Cu(OH)_4^{2-}$; (b) 50 mM $[Ni^{2+}(CN)_4]$; (c) 50 mM $Cu^{2+}[Ni^{2+}(CN)_4]$ (Cu to Ni ratio 1:4). Electrolysis conditions: Electrodes (4 cm^2) = Pt (anode) and anodized Ti (cathode); Current density – 30 mA cm^{-2}; Solution flow rate = 70 ml min^{-1}. Inset figure shows formation of Cu^{1+} from $Cu^{2+}[Ni^{2+}(CN)_4]$ during electrolysis at the above conditions.

Fig.3 ESR spectra of frozen $Cu^{2+}[Ni^{2+}(CN)_4]$ in 10 M KOH solution (a) before and (b) after electrolysis. Electrolysis conditions are the same as in legend of Fig.2.

Fig.4 CF_4 removal efficiency variation during electro-scrubbing by scrubbing solution of electrolyzed $Cu^{2+}/Cu^{1+}[Ni^{2+}(CN)_4]^{1-/0}$ solution. Conditions: Feed concentration of CF_4 = 10 ppm; Gas flow rate = 0.2 L min^{-1}; Scrubbing solution flow rate = 3 L min^{-1}. Solution flow rate to electrolytic cell = 2 L min^{-1}; Electrodes area = 50 cm^2. Inset figure shows electrogenerated $Cu^{1+}[Ni^{2+}(CN)_4]^{1-}$ concentration variation during removal of CF_4 pollutant.

Fig.5 (A) Effect of gas flow rate (mentioned in the figure) with time on removal of CF_4 using electrogenerated $Cu^{1+}[Ni^{2+}(CN)_4]^{1-}$ in 10 M KOH solution at electro-scrubbing. Remaining experimental conditions are same as in the legend of Fig.4

(B) Effect of CF_4 feed concentration variation with time on it's removal by electrogenerated $Cu^{1+}[Ni^{2+}(CN)_4]^{1-}$ in 10 M KOH solution at electro-scrubbing. Remaining experimental conditions are same as in the legend of Fig.3.

Fig.6 Online FTIR gas analyzer results of exit gas products (mentioned in the figure) during CF_4 removal at electro-scrubbing by electrogenerated $Cu^{1+}[Ni^{2+}(CN)_4]^{1-}$ in 10 M KOH solution at electro-scrubbing. Remaining experimental conditions are same as in the legend of Fig.4.

Fig.7 Subtracted (from before and after electro-scrubbing) solution phase offline ATR-FTIR spectrum for the product formed in the solution during removal of CF_4. The experimental conditions are same as in the legend of Fig.4.

Figures

Fig.1

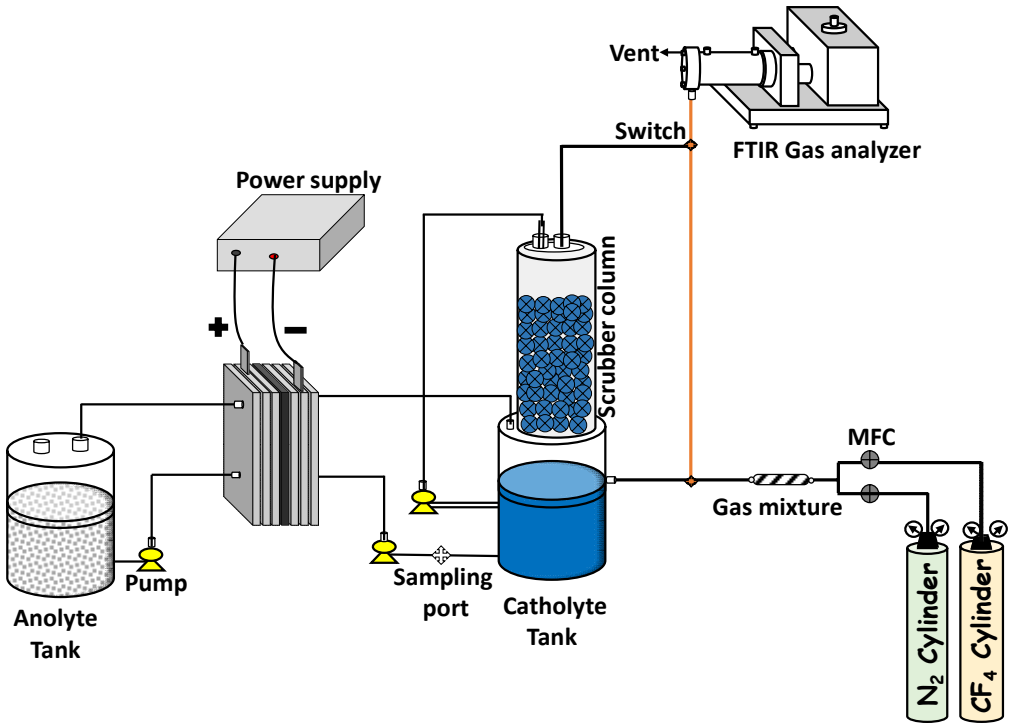

Fig.2

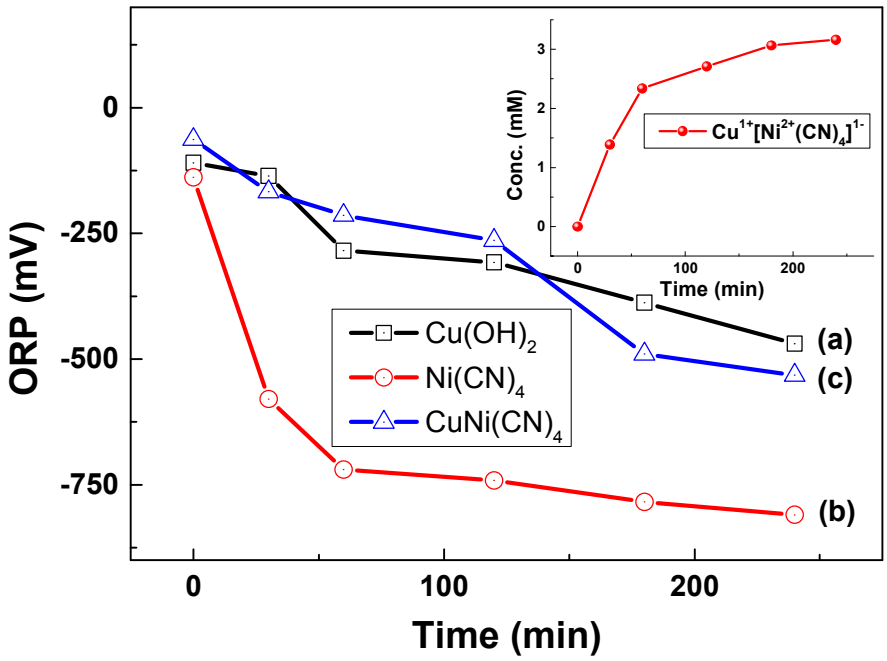
ORP (mV)
0
-250
-500
-750
0
100
200
Time (min)
Cu(OH)2
Ni(CN)4
CuNi(CN)4
(a)
(c)
(b)
Conc. (mM)
3
2
1
0
0
100
200
Time (min)
Cu1+[Ni2+(CN)4]1-

Fig.3

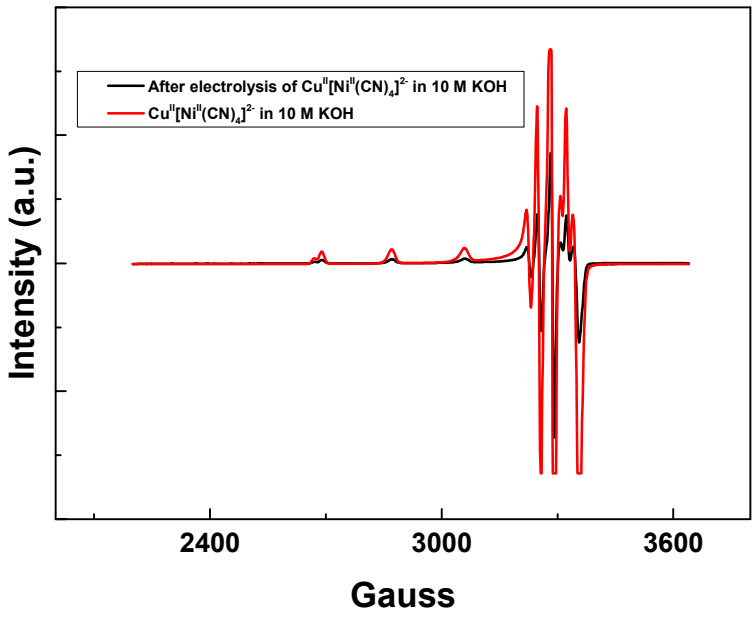
After electrolysis of $Cu^{II}[Ni^{II}(CN)_4]^{2-}$ in 10 M KOH
$Cu^{II}[Ni^{II}(CN)_4]^{2-}$ in 10 M KOH
Intensity (a.u.)
2400
3000
3600
Gauss

Fig.4

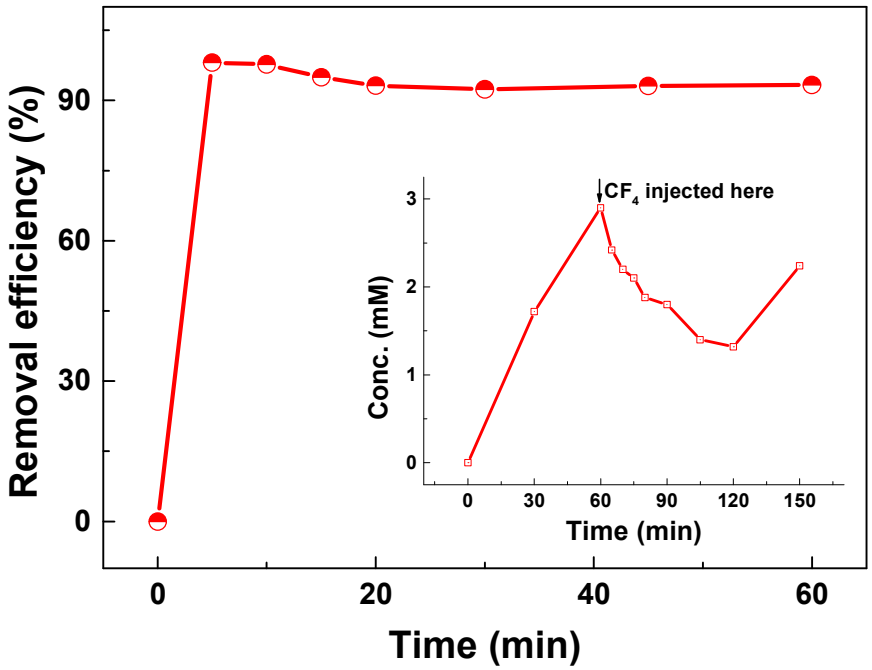
Removal efficiency (%)
0
30
60
90
0
20
40
60
Time (min)
Conc. (mM)
0
1
2
3
0
30
60
90
120
150
Time (min)
CF4 injected here

Fig.5

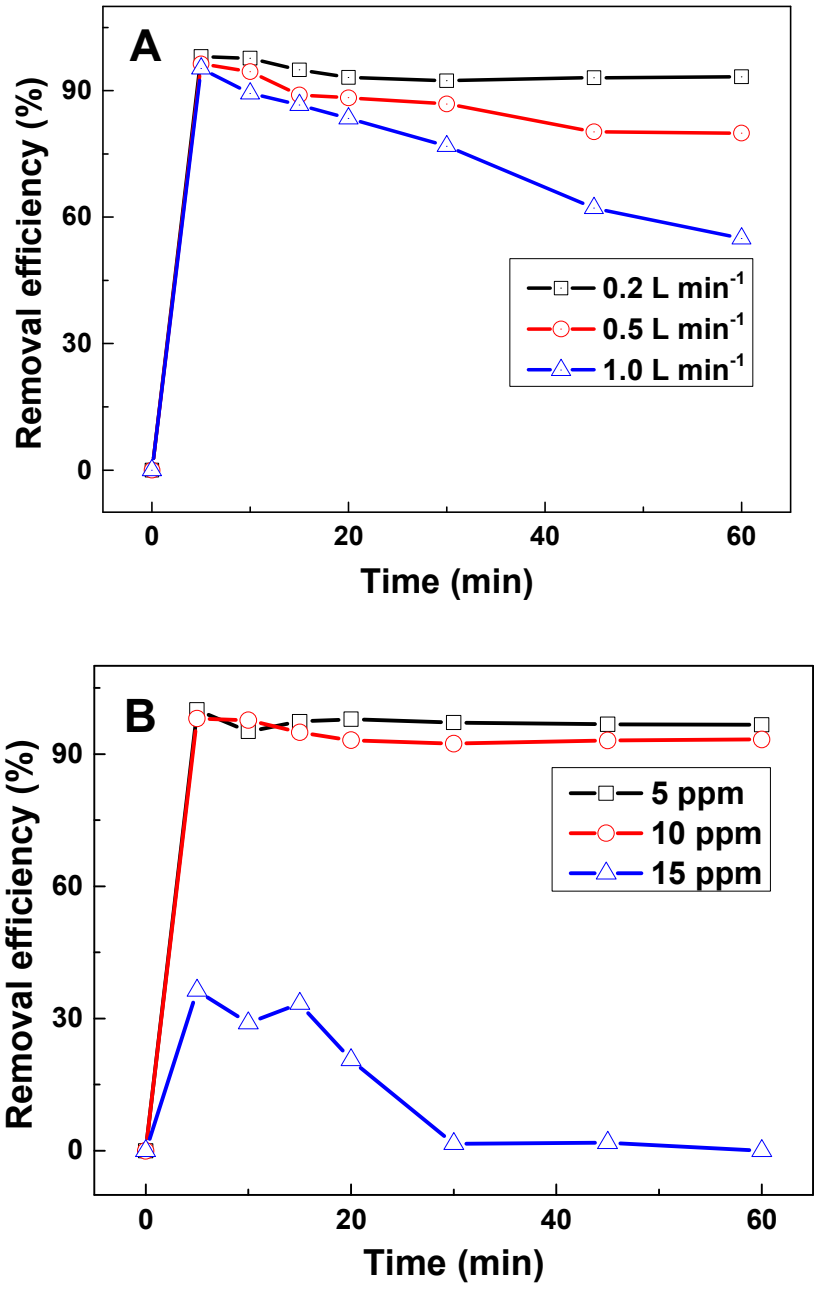
A
Removal efficiency (%)
0
30
60
90
0
20
40
60
Time (min)
0.2 L min-1
0.5 L min-1
1.0 L min-1
B
Removal efficiency (%)
0
30
60
90
0
20
40
60
Time (min)
5 ppm
10 ppm
15 ppm

Fig.6

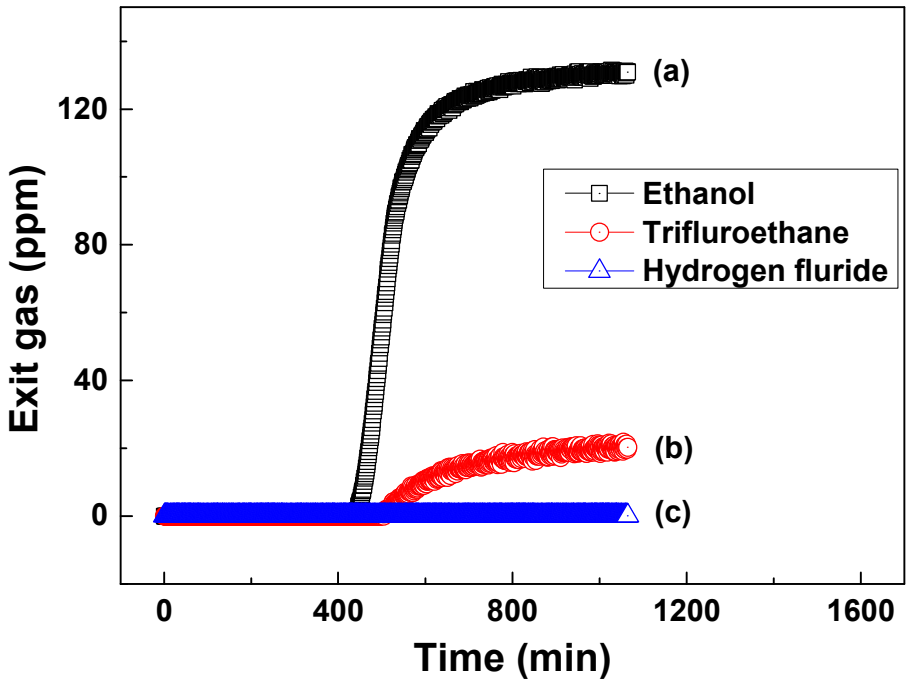
Exit gas (ppm)
120
80
40
0
0
400
800
1200
1600
Time (min)
(a)
(b)
(c)
Ethanol
Trifluroethane
Hydrogen fluride

Fig.7

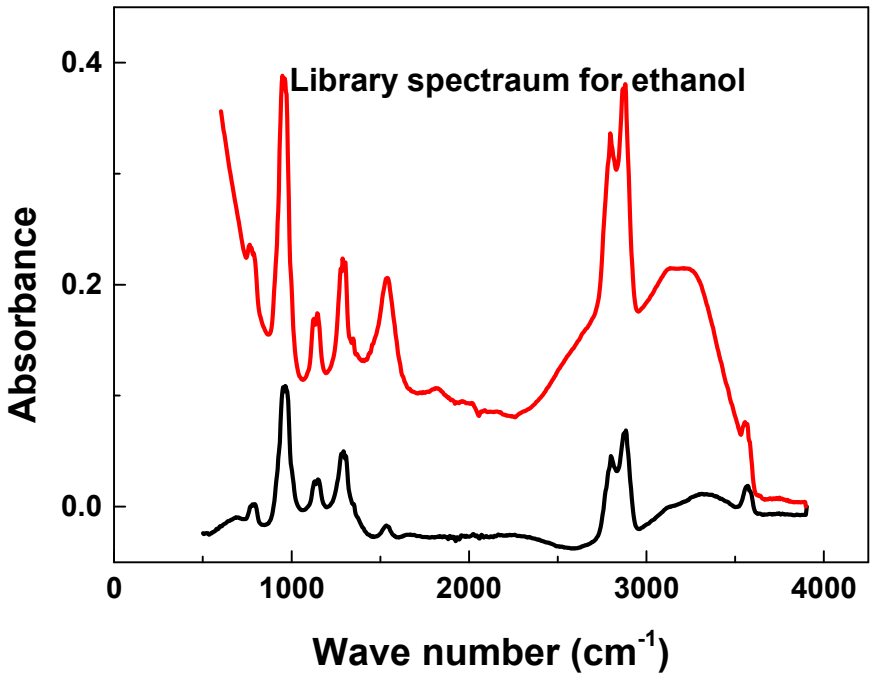
Library spectraum for ethanol
Absorbance
0.4
0.2
0.0
0
1000
2000
3000
4000
Wave number (cm-1)